In the Proceedings of the 1997 American Controls Conference in
Albuquerque, NM, June 3-6 1997.

# Decomposition of Baseline Noise Sources in Hard Disk Position Error Signals Using the PES Pareto Method

Daniel Abramovitch
*Hewlett-Packard Laboratories*
*1501 Page Mill Road, M/S 2U-10*
*Palo Alto, CA 94304*
E-mail: danny@hpl.hp.com

Terril Hurst
*Hewlett-Packard Laboratories*
*1501 Page Mill Road, M/S 2U-10*
*Palo Alto, CA 94304*
E-mail: terril@hpl.hp.com

Dick Henze
*Hewlett-Packard Laboratories*
*1501 Page Mill Road, M/S 2U-10*
*Palo Alto, CA 94304*
E-mail: Dick_Henze@hpl.hp.com

**Abstract**– This paper uses the PES Pareto Method[1] and measurement techniques for isolating noise sources[2] to decompose the Position Error Signal (PES) of a Lynx II hard disk drive manufactured by Hewlett-Packard. This accomplishes three things: it demonstrates the utility of the PES Pareto Method in a practical example, it allows us to discover which noise sources are insignificant to PES, and it identifies which noise sources are significant to PES. In this particular hard disk drive, it is discovered that the two most significant sources of baseline noise at the disk's position error signal are the turbulent wind flow generated by the spinning disks (Windage) and the noise involved in the actual readback of the Position Error Signal (Position Sensing Noise).

## 1. Introduction

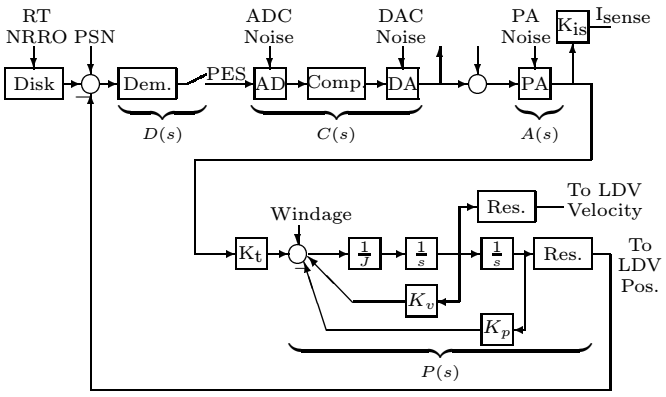


Figure 1: Generalized view of track following model.

In a companion paper[1], a method is presented for separating the the contributors of various sources of uncertainty ("noises") in the postion error signal (PES) of the track-follow servo in a disk drive. In a second paper[2], specific measurements are made to isolate individual noise sources and to create appropriate filters from which the noises can be examined at their source and at PES. This third paper completes the process by using the method in the former and the measurements in the latter to feed the appropriate spectra through the appropriate loop filters to yield both the input noise spectra and their effect – both individually and cumulatively – on PES. The PSDs are then integrated in frequency to yield the corresponding power spectra and variances.

A hard disk drive's Position Error Signal (PES) can be decomposed in the frequency domain into three components:

**Synchronous or Repeatable Excitation:** This is typically due to the rotation of the spindle and therefore synchronous with it or one of the spindle orders. While synchronous excitation may be large, it is already standard practice in the disk drive industry to use feedforward cancellers to dramatically attenuate its effect[3, 4].

**Non-synchronous or Non-repeatable Spectral Excitation:** While this excitation does not correspond to any of the spindle orders, it does have sharp spectral peaks due to cage orders. Typical sources of this excitation are disk or arm resonances (which are less sharp but still narrow band), often stimulated by synchronous or broadband excitation. Again, this can have a significant effect on PES, however, it has become recently apparent that such phenomena as disk resonances can be considerably reduced by the use of damped substrates[5, 6].

**Broadband or Baseline Noise:** This is the broad baseline level of the noise that remains when all the narrow band components have been removed. Of these three categories, it is the hardest to disect and therefore the hardest one to for which to find solutions.

In order to achieve very high track densities, each of these sources of PES must be reduced considerably. For the first two, it appeared that reasonable engineering solutions should be available. However, the baseline noise was more nefarious and therefore of these three categories of noise in PES, it was the one singled out for this work. The PES Pareto Method[1] and the measurement techniques for noise source isolation[2] to isolate the building blocks of the PES baseline were used. The reasoning was that understanding the building blocks of the baseline noise, would allow solutions that worked on those building blocks.

> When you have eliminated the impossible, whatever remains, *however improbable* must be the truth.
> — *Sherlock Holmes[7]*

The above quotation holds in it the key philosophy of the PES Pareto Method: eliminate all the impossible, observe what is left, and from there determine the true sources of noise in a disk drive's Position Error Signal (PES). To recap what was described in the two previous papers[1, 2], the method involves four distinct steps:

- isolate measurement of noise source ("common mode reject"),
- filter backwards to obtain the PSD of the noise source,
- filter forwards to obtain the effect of this particular noise on the PES PSD, and

- compare these PSDs at PES to each other and add them to cumulative PES PSD.

The map for this analysis is the system block diagram shown in Figure 1. A more detailed version of this is shown in the method paper[1]

This paper will apply this method to a set of noise source isolation measurements described in [2] to finally uncover the relative significance to PES of each noise source. The paper has the following organization. Section 2 goes through each individual measured noise source both at the source and at PES. Section 3 puts these together at PES. Section 4 then shows a small subset of what can be extrapolated from these results. Some conclusions are presented in Section 5. Throughout this paper, the term "the method paper" will refer to the paper describing the PES Pareto Method[1] and "the measurement paper" will refer to the noise source isolation measurement paper[2].

## 2. Individual Noise Sources

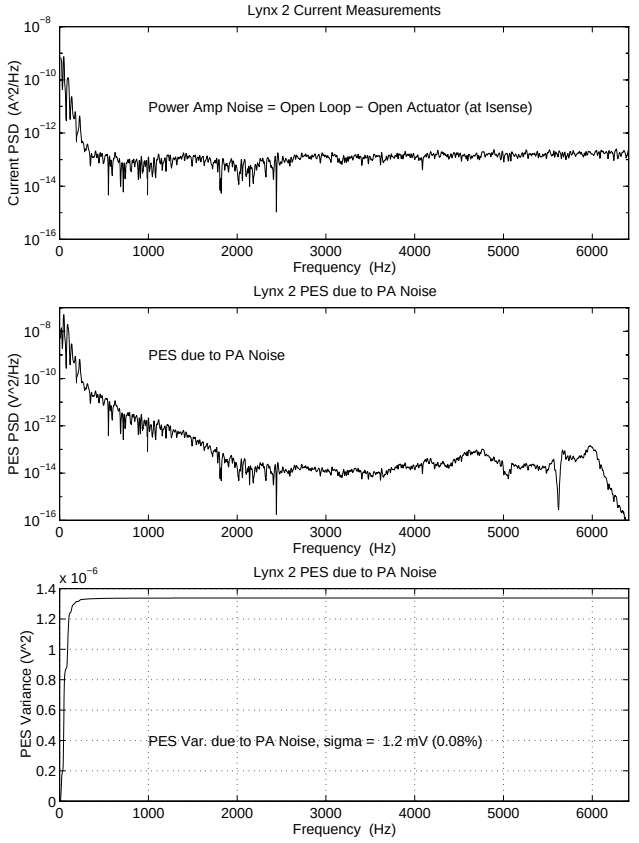


Figure 2: Power Amp Noise PSD

In this section, we will briefly present the results obtained when the measurements to isolate a noise source[2] are then filtered back to the noise source input and then forward to PES.

**2.1 Power Amplifier:** The power amplifier noise is measured directly at $I_{sense}$. This measurement is made with the loop open, so no loop unwrapping is necessary. Furthermore, the power amplifier noise is modeled to enter the system right in front of $I_{sense}$. Thus, the backwards filter to the source is simply unity (1) and the forward filter from the source noise PSD to PES PSD is

$$\left\| \frac{K_t P(s) D(s)}{1 + K_t P(s) D(s) C(s) A(s)} \right\|^2 .$$

Note from Figure 2 that power amp noise is only significant at low frequency.

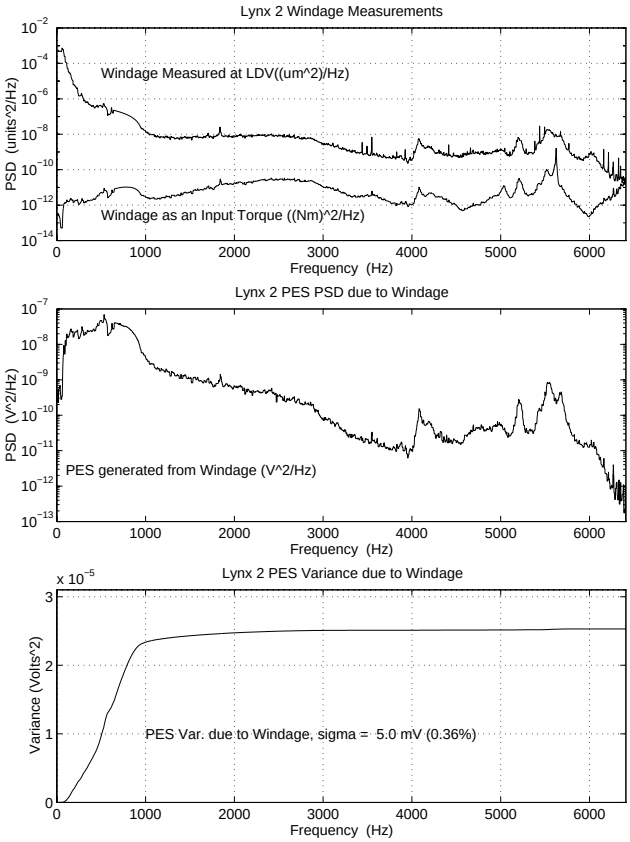


Figure 3: Windage PSD

**2.2 Windage:** Windage is measured using the Laser Doppler Vibrometer (LDV) to measure the velocity of the readback head and then integrate it in time for the head position. (For frequencies above 10 Hz, this is considered more accurate than using a direct position measurement scheme.) The Windage is the difference between the head motion when the drive actuator is electrically disconnected from the power amp but the disk is spinning and the same measurement when the disk is stopped. In the former case, it can take several iterations to find a spot where the head will sit comfortably in order to make a reasonable measurement. Given that the measurement is made, the filter back to the source is given by

$$\left\| \frac{1}{P(s)} \right\|^2 ,$$

and the filter forward from the source to PES is

$$\left\| \frac{P(s) D(s)}{1 + K_t P(s) D(s) C(s) A(s)} \right\|^2 .$$

Note that the effect of Windage as shown in Figure 3 is most significant below 1 kHz.

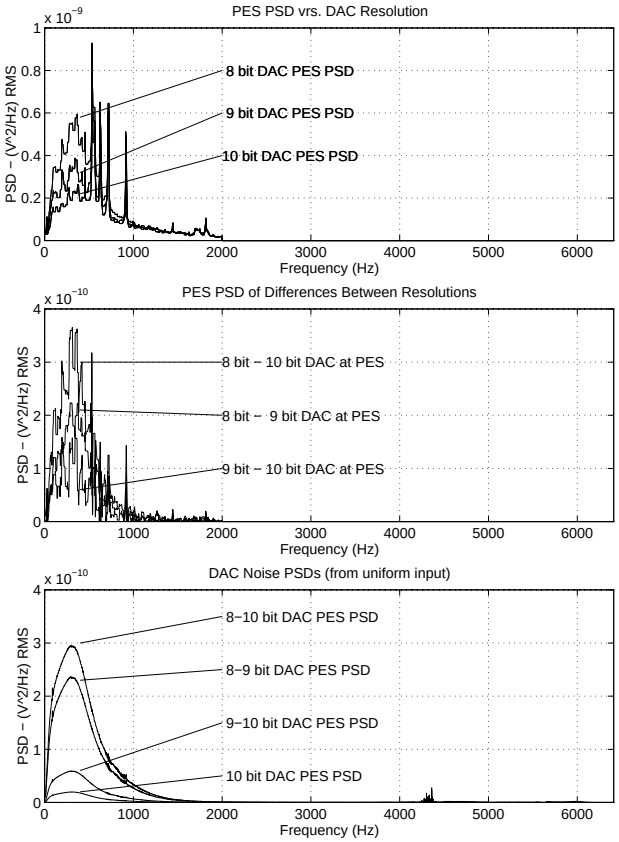


Figure 4: DAC Noise PSD

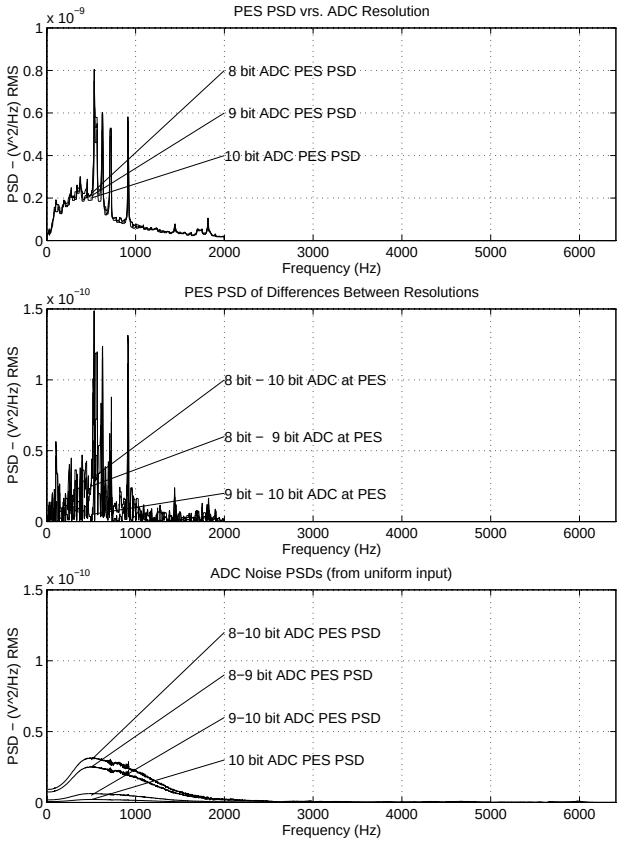


Figure 5: ADC Noise PSD

**2.3 DAC Noise:** In order to measure the effects of quantization on the PES PSD, bits were artificially masked off in the drive DSP and then the PES PSD was recorded. In order to isolate out the noise due to the DAC quantization the measurements of PES PSD with a 10 bit DAC was subtracted from the the PES PSD with a 9 bit DAC. This gave the effect of losing that one bit of quantization. The same operation was repeated with the 8 bit DAC PES PSD - 9 bit DAC PES PSD and 8 bit DAC PES PSD - 10 bit DAC PES PSD.

However, due to the extremely small levels of these signals, these differences themselves were quite noisy. Filtering them backwards from PES to the DAC only amplified the noise. Thus, the previous method was ineffective. Instead, the standard uniform white noise model was used as an input PSD to the DAC. The difference between different quantizer levels could then be filtered forward to PES using the filter

$$\left\| \frac{K_t P(s) D(s) A(s)}{1 + K_t P(s) D(s) C(s) A(s)} \right\|^2 = \left\| \frac{C(s)}{T_{cl}} \right\|^2,$$

which essentially matched the shape of measured differences. The level of the input DAC noise was then scaled to get an effective level of

$$q = \frac{0.3125\ V}{512\ counts} * \frac{1}{9}$$

which was $\frac{1}{9}$ the level one would calculate from the system model. The PES noise generated by the Lynx II's 10 bit DAC is derived in this way and shown in the bottom plot of Figure 4.

**2.4 ADC Noise:** The problems encountered with backwards filtering DAC noise measurements were even worse with ADC noise measurements. However, using the same method as was done for the DAC noise measurements, yielded a uniform white noise input PSD forward filtered from the ADC to PES using

$$\left\| \frac{K_t P(s) D(s) C(s) A(s)}{1 + K_t P(s) D(s) C(s) A(s)} \right\|^2 = \left\| \frac{1}{T_{cl}} \right\|^2$$

which was then adjusted in amplitude to obtain an input quantization of

$$q = \frac{1.25\ V}{512\ counts} * \frac{1}{20}$$

or $\frac{1}{20}$ of the ADC noise one would obtain from the nominal system model. The PES nosie generated by the Lynx II's 10 bit ADC is derived in this way and shown in the bottom plot of Figure 5. Note that its effect on PES is even lower than that of the DAC.

## 3. Putting It All Together at PES

Given that most of the individual noise sources and their effects on PES have been identified, they can now compared individually or stacked up cumulatively as shown in Figure 6. (The latter is shown since the stacking of the PSDs and variances makes is more readable than lines which criss-cross.)

Note that even though most of the potential sources shown in the small block diagram of Figure 1 and described in detail in the method paper[1] have been accounted for, there is still a significant portion of the baseline PES PSD that is unaccounted for, especially at high frequencies. This is especially obvious in the cumulative variance plot in Figure 6. If

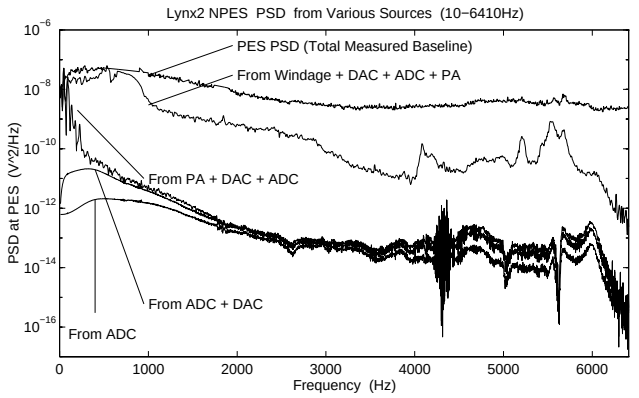


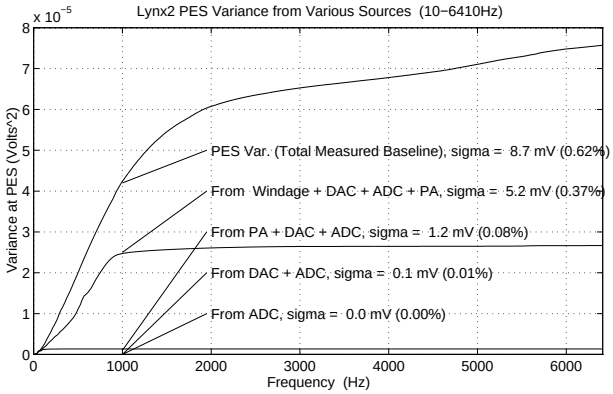


Figure 6: Cumulative Noise Source PSDs at PES

one zooms in on the total baseline PES PSD and subtracts off what has been accounted for one gets a curve which very much looks like a scaled version of

$$\|D(s)S_{cl}(s)\|^2 = \left\| \frac{D(s)}{1 + K_t P(s)D(s)C(s)A(s)} \right\|^2$$

as shown in Figure 7. This tends to indicate a noise which is injected at the reference input, and the two possibilities here for non-repeatable baseline noise are Real Time Non-Repeatable Run Out (RT NRRO) and Position Sensing Noise (PSN). By filtering the "what's left" curve back to the input by

$$\left\| \frac{1}{D(s)S_{cl}(s)} \right\|^2$$

then a very interesting result drops out as shown in Figure 8. Note that there is a broadband, essentially white noise component to "what's left". There is also a large hump at low frequency. As Windage is accounted for already, the most likely source of this large hump is the actual non-repeatable motion of the disk on the rotating spindle (RT-NRRO). Likewise the broadband flat noise cannot be from the power amplifier, ADC, or DAC (since these have been eliminated) and therefore it follows that this is Position Sensing Noise. If this PSD is fed forward to PES and then integrated in frequency to yield the PES baseline variance due to PSN, this number, $\sigma_{PSN} = 0.03\mu m$, closely matches the prediction of the ANOVA analysis[2].

## 4. Extrapolations

At this point, we have made use of all of our measurements and must now do some deduction from what is left. If in fact,

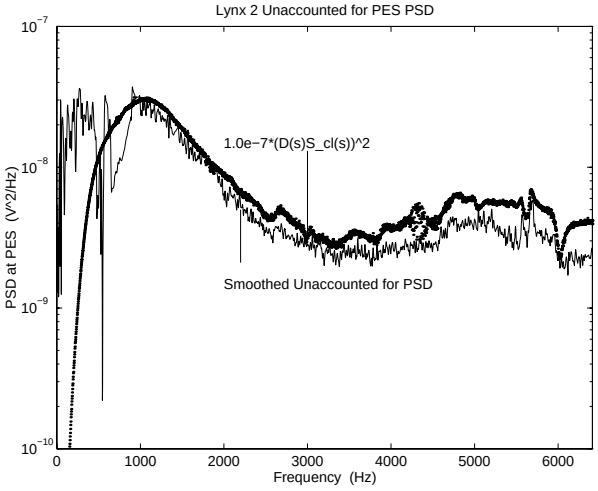


Figure 7: Unaccounted for Noise at PES

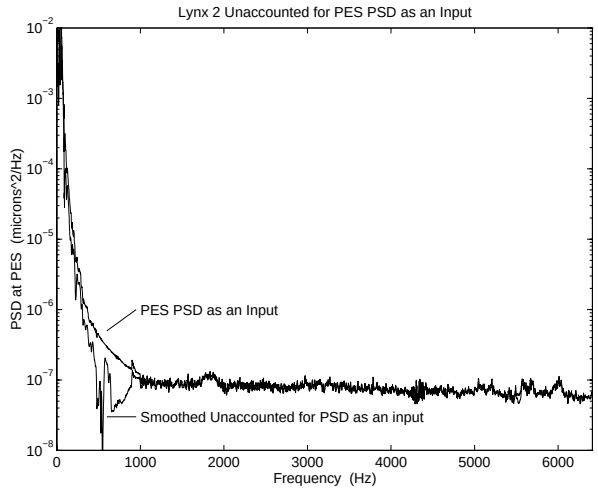


Figure 8: Unaccounted PES Noise as an Input

the PSN is white, then we can extrapolate back from the flat portion of the curve in Figure 8. Calling this PSN, we can then subtract this value from the "what's left" input PSD to obtain the PSD of the Real Time NRRO.

Given that we have isolated the "white" PSN input, we can now do some modeling experiments where we alter the level of the PSN to observe the effect on the overall level of baseline PES. With the spindle rotating at the nominal speed of 5400 rpm, the results are shown in Figure 9.

Likewise, having isolated Windage's contribution allows us to examine the effect of increased windage on the overall PES baseline. As Windage was something we could actually measure, the spindle speed was adjusted using a special spindle controller board to allow measurement of Windage for spindle speeds of 3600, 5400, 7200, and 9600 RPM. The measurement results are shown in the measurement paper[2]. The procedure for feeding these Windage PSDs back to the source and forward to PES is identical to what has been done at the nominal spindle speed of 5400 RPM. It is useful to look at the overall PES variance due to Windage with changing RPM, and this is shown in Figure 10. Note that the increase in baseline PES variance is *not* linear with spindle speed, but in fact grows dramatically at the higher RPMs. This is significant as newer high performance drives spin at 7200 RPM and beyond.

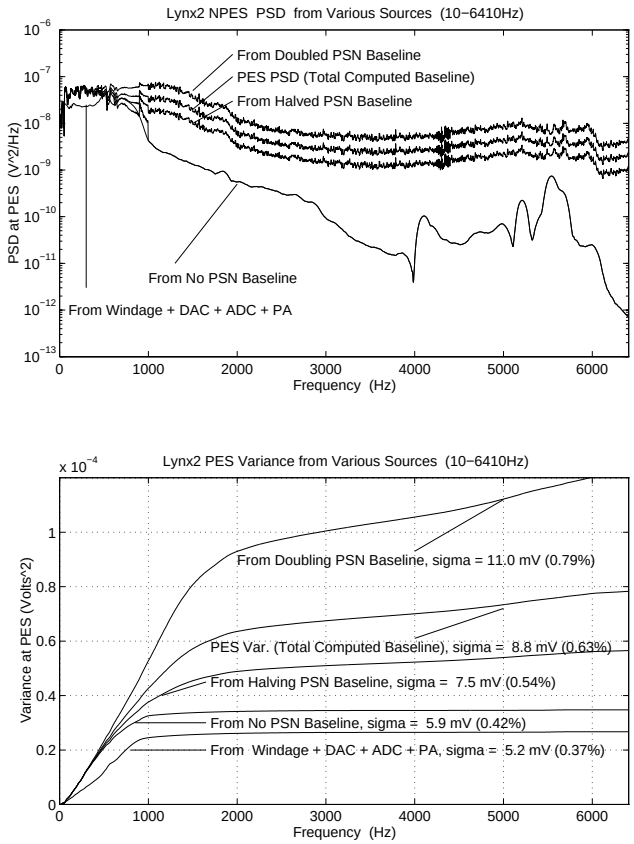


Figure 9: Effect of Changing Baseline PSN (5400 rpm)

## 5. Conclusions

What should be apparent now is that in this particular disk drive there are essentially two main sources of baseline noise in PES. The first is the Windage which is responsible for approximately one third of the total measured baseline PES variance. Windage has an effect primarily at low frequency (below 1 KHz). The second major contributor is Position Sensing Noise (PSN). PSN is flat at the input, but is shaping by the loop so that it has a rapid ramp up at low frequency and then tapers to a constant level at high frequency. However, because of the broadband nature of this noise, its effect dominates the higher frequencies (above 1 kHz).

Furthermore, these noises are tied together through the loop behavior in a way described by Bode's Integral Theorem[8]. Any attempt to drive down the PES variance caused by Windage through increased loop bandwidth results in an amplification of PSN by the loop. Minimizing the bandwidth so as not to amplify PSN probably means that the Windage is not adequately attenuated. The situation only gets worse as the spindle RPM goes up, driving up the level of Windage and therefore requiring more loop bandwidth. This greater bandwidth *must* increase the amplification of PSN.

In this context it becomes clear that two distinct efforts will yield a lower baseline PSD for PES. The first effort is to carefully study the wind flow within a disk drive to find ways to minimize the level of Windage noise. This is a nontrivial task involving the study of turbulent air flows[9]. The second effort is to find ways to minimize PSN. This can be accomplished via improving the readback process and/or the demodulation process. Research is currently being done on the former[10]. It

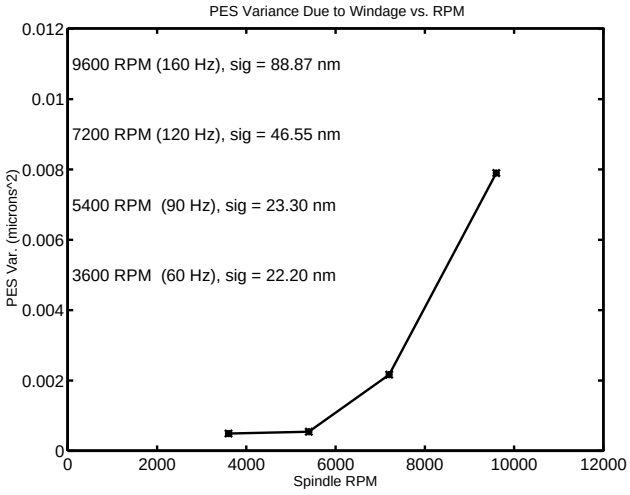


Figure 10: PES Variance Due to Windage Versus RPM

is possible that the best answer might require an entirely new position sensing method. Recognizing the significant effect that PSN has on overall baseline PES allows us to justify such an effort.

## References


[1] D. Abramovitch, T. Hurst, and D. Henze, "The PES Pareto Method: Uncovering the strata of position error signals in disk drives," in *Submitted to the 1997 American Control Conference*, (Albuquerque, NM), AACC, IEEE, June 1997.

[2] T. Hurst, D. Abramovitch, and D. Henze, "Measurements for the PES Pareto Method of identifying contributors to disk drive servo system errors," in *Submitted to the 1997 American Control Conference*, (Albuquerque, NM), AACC, IEEE, June 1997.

[3] A. Sacks, M. Bodson, and W. Messner, "Advanced methods for repeatable runout compensation (disc drives)," *IEEE Transactions on Magnetics*, vol. 31, August 1994.

[4] M. Bodson, A. Sacks, and P. Khosla, "Harmonic generation in adaptive feedforward cancellation schemes," *IEEE Transactions on Automatic Control*, vol. 39, September 1994.

[5] J. S. McAllister, "The effect of disk platter resonances on track misregistration in 3.5 inch disk drives," *IEEE Transactions on Magnetics*, vol. 32, pp. 1762–1766, May 1996.

[6] J. S. McAllister, "Characterization of disk vibrations on aluminum and alternate substrates," *IEEE Transactions on Magnetics*, January 1997. To appear.

[7] S. A. C. Doyle, *The Sign of Four*. 1890.

[8] H. W. Bode, *Network Analysis and Feedback Amplifier Design*. New York: Van Nostrand, 1945.

[9] H. Suzuki and J. A. C. Humphrey, "Flow past large obstructions between corotating disks in fixed cylindrical enclosures," in *Proceedings of the ASME IMECE Conference*, (Atlanta, GA), ASME, August 1996.

[10] P. Mathur, "Position signal generation on magnetic disc drives." Ph.D. Thesis Proposal at CMU, May 1996.